JCTC Journal of Chemical Theory and Computation

pubs.acs.org/JCTC Letter

Quantum Computer Simulation of Protein Protonation

Hao Hu*

Cite This: J. Chem. Theory Comput. 2023, 19, 5671−5676 Read Online

ACCESS | Metrics & More | Article Recommendations | Supporting Information

ABSTRACT: In attempts to simulate the protonation of proteins, a major challenge is that the number of protonation states grows rapidly as a function (2^N) of the number of protonation sites (N). Expression on the free energy of the protonation state as an N-site Ising model — using an empirical Generalized-Born model — allows a quantum computer to efficiently determine the important states at a given pH value and subsequently reconstruct the pH titration process at all sites. Compared with the exact results painstakingly obtained with classical computers, the results obtained using quantum computers show good agreement for staphylococcal nuclease and excellent agreement for α-lactalbumin. This work illustrates the effectiveness of quantum computers in sampling important physical states, which may be useful in attacking challenging biomolecular problems.

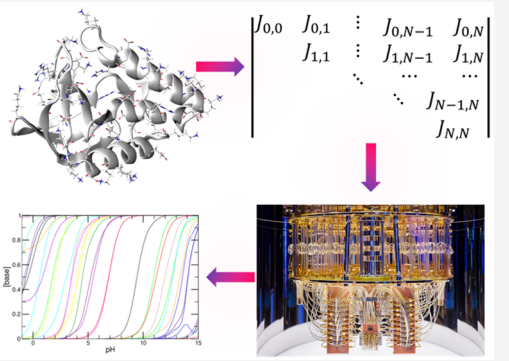

Protonation and proton transfer play critical roles in the stability, function, and regulation of biomolecular processes.[1−4] Since protonation and deprotonation can drastically change the electrostatic properties of the target group, as such the term "ionization" is often used to reflect the net charge change, a combination of multiple protonation groups in protein and other biomolecules provides a convenient and often refined means to stabilize the protein structure and achieve the delicate functions.[5−8] The physical chemistry of the ionization processes has attracted great attention from the very early biochemical researchers[9] and remains to be an intensively studied topic today.[10,11]

Theoretical study of protein protonation faces several technical challenges. These include, but are not limited to,[12−15] a method to accurately compute the bond formation/dissociation energy; an energy function to accurately describe the solvation effect; sufficient phase space samplings to take into account the contribution of the protein conformational fluctuations; and last but not least, the site−site coupling between different protonation groups that creates a large number of different ionization/protonation states. The total number of protonation states grows as quickly as 2^N. As a result, usually only a small number of ionization sites could be studied in conventional simulations even with the enhanced sampling methods such as the constant pH molecular dynamics simulation[16−18] or the generalized ensemble method.[14]

Breaking the number barrier of protonation states calls for unconventional computation methods. In recent years, the fast development of modern quantum computers, including quantum annealers, provides new opportunities to efficiently attack an array of complex problems in chemistry, notably in the field of electronic structure and statistical mechanics. The computational costs of these problems usually scale as the power or exponential functions of the system size or dimension and thus quickly outpace the capacity of traditional computers[19] — within conventional computing framework they must be solved with truncation or reduction of the problem's complexity.[20] Development in quantum computers creates a new paradigm to study them directly.

As the application of quantum computers to the chemistry field is still in its infancy, identifying proper chemistry problems to demonstrate the usability, correctness, and power of quantum computers would facilitate the broader application of quantum computers in the chemistry field. The protein ionization process, especially the site−site coupling issue, is one such important problem that fits naturally to the application scope of quantum computers.

Each ionizable group in protein molecules possesses two different electrostatic states, protonated and deprotonated, with each state interacting very differently from other ionizable groups to form a distinctive thermodynamic state. Therefore, the number of possible thermodynamic states is 2^N for N-ionizable sites. It is more convenient and rigorous to consider all of the thermodynamic states together statistically as a grand canonical ensemble. The protonation state of each site may be denoted with a binary variable as

Received: June 7, 2023
Published: August 9, 2023

https://doi.org/10.1021/acs.jctc.3c00606
J. Chem. Theory Comput. 2023, 19, 5671−5676

$$\lambda_i = \begin{cases} 0 & \text{protonated} \\ 1 & \text{deprotonated} \end{cases} \quad i = 1, 2, ..., N \tag{1}$$

For the convenience of discussion later, here state 0 is designated as protonated. Each protonation state, characterized by protonation of individual sites $\{\lambda_1,\lambda_2,...,\lambda_N\}$, is a distinct thermodynamic state with the free energy $A(\{\lambda_1,\lambda_2,...,\lambda_N\})$. The grand canonical partition function of the protein molecule at a given pH is[21]

$$\Xi(\text{pH}) = \sum_{\{\lambda_1,\lambda_2,...,\lambda_N\}} \exp(-\beta A(\{\lambda_1, \lambda_2, ..., \lambda_N\}))\mu^{n_i} \tag{2}$$

where β is the inverse of the product of Boltzmann constant k and temperature T, and μ is the exponential of the chemical potential of the proton in solution

$$\mu = \exp(-\ln 10 \times \text{pH}) \tag{3}$$

The proton occupation number n_i is

$$n_i = \sum_{j=1}^{N} (1 - \lambda_j) \tag{4}$$

The summation in the partition function runs over all 2^N states of $\{\lambda_1,\lambda_2,\cdots,\lambda_N\}$. The protonation probability of an ionization site m is computed as an expectation value as

$$P_m(\text{pH}) = 1 - \frac{\sum_{\{\lambda_1,...\lambda_m...,\lambda_N\}} \lambda_m \exp(-\beta A(\{\lambda_1, ...\lambda_m..., \lambda_N\}))\mu^{n_i}}{\Xi(\text{pH})} \tag{5}$$

The change of protonation probability with respect to the pH value could be plotted as a virtual titration curve for the given sites.[14]

The free energy of each protonation state, $A(\{\lambda_1,\lambda_2,\cdots,\lambda_N\})$, may decompose into two contributions. The first term is the solvation free energy of the protein molecule at a given protonation state. The second term is the quantum mechanical energy change associated with the *X-H* bond breaking/formation.[12] The two terms are obtained with different approximations in this work, allowing us to derive a simple Ising model to tackle this problem. The theoretical details are provided in the Supporting Information.

The Generalized Born (GB) model[22] is used to compute the solvation free energy in the current work. We express the atomic charges in a protonation-dependent form: the atomic charge of an atom i in an ionizable group m is q_i^A for the acidic form and q_i^B for the basic form, which can be combined as

$$q_i(\lambda_m) = q_i^A + \lambda_m \Delta q_i = \begin{cases} q_i^A & \lambda_m = 0 \\ q_i^B & \lambda_m = 1 \end{cases} \tag{6}$$

with

$$\Delta q_i = q_i^B - q_i^A \tag{7}$$

The interaction between two atoms, i in an ionizable group m and j in an ionizable group n, may be expressed in the Generalized Born form, but without the self-interaction energy, as

$$f_{GB}(q_i(\lambda_m), q_j(\lambda_n)) = f_{GB}(q_i^A, q_j^A) + \lambda_m f_{GB}(\Delta q_i, q_j^A) + \lambda_n f_{GB}(q_i^A, \Delta q_j) + \lambda_m\lambda_n f_{GB}(\Delta q_i, \Delta q_j) \tag{8}$$

This can be further extended to the solvation free energy of the whole protein molecule including both the N ionizable groups and the rest of the nonionizable groups of the protein.

The quantum mechanical contribution of the formation/dissociation of an *X-H* bond could be computed theoretically.[12,15] However, here, it is derived as a bonding-correction free energy term that is obtained using both the experimental pK_a value and the GB model of the cognate model molecules. This approach in fact greatly improves the overall performance of the model as similar ideas have long been used in theoretical study of enzyme reactions.[23] Considering a single ionizable group in solution undergoing the protonation equilibrium,

$$XH_{aq} \rightleftharpoons X_{aq}^- + H_{aq}^+ \tag{9}$$

the bonding-correction term is

$$\Delta U_{corr} = kT \ln 10 \times \text{p}K_a - U(X^-) + U(XH) \tag{10}$$

where U is the solvation free energy of the cognate model compound in the specified protonation state computed using the same GB model as in the previous discussion.

The final free energy of a protonation state is

$$\begin{aligned} A = &\sum_m \lambda_m \Delta U_{corr,m} + \sum_m \sum_{\substack{i\in m \\ j\in P}} f_{GB}(q_i^A, q_j) + \sum_m \lambda_m \sum_{\substack{i\in m \\ j\in P}} f_{GB}(\Delta q_i, q_j) \\ &+ \sum_{m<n} \sum_{\substack{i\in m \\ j\in n}} f_{GB}(q_i^A, q_j^A) + \sum_{m\neq n} \lambda_m \sum_{\substack{i\in m \\ j\in n}} f_{GB}(\Delta q_i, q_j^A) \\ &+ \sum_{m<n} \lambda_m\lambda_n \sum_{\substack{i\in m \\ j\in n}} f_{GB}(\Delta q_i, \Delta q_j) + \frac{1}{2} \sum_m \sum_{i,j\in m} f_{GB}(q_i^A, q_j^A) \end{aligned} \tag{11}$$

Note the simplification made using $\lambda_m^2 = \lambda m$. This can be combined into the grand canonical partition function as

$$\begin{aligned} \Xi(\text{pH}) = \sum_{\{\lambda_1,\lambda_2,...,\lambda_N\}} \exp\Bigg(-\beta\Bigg[&\sum_m \sum_{\substack{i\in m \\ j\in P}} f_{GB}(q_i^A, q_j) + \sum_{m<n} \sum_{\substack{i\in m \\ j\in n}} f_{GB}(q_i^A, q_j^A) + \frac{1}{2} \sum_m \sum_{i,j\in m} f_{GB}(q_i^A, q_j^A) \\ &+ \sum_m \lambda_m \Bigg((\Delta U_{corr,m} - kT \ln 10 \times \text{pH}) + \sum_{\substack{i\in m \\ j\in P}} f_{GB}(\Delta q_i, q_j) + \sum_{\substack{i\in m \\ j\in n}} f_{GB}(\Delta q_i, q_j^A) \Bigg) + \sum_{m<n} \lambda_m\lambda_n \sum_{\substack{i\in m \\ k\in n}} f_{GB}(\Delta q_i, \Delta q_k) \Bigg]\Bigg) \end{aligned} \tag{12}$$

All states can then be enumerated on classical computers without further approximations but with the caveat that it is

https://doi.org/10.1021/acs.jctc.3c00606
J. Chem. Theory Comput. 2023, 19, 5671−5676

extremely expensive to do so for a big number of states, even with the embarrassing parallelism between the computation of states.

Instead of exhaustive enumeration, one may use quantum annealing to determine the important protonation states and derive the protonation properties from these sampled states. A quantum annealer takes advantage of the quantum annealing method.[24−26] In quantum annealers, the system Hamiltonian adiabatically evolves from a tunneling Hamiltonian to the target Hamiltonian, so that the system ends classically in the most-favorable states or regions. In most systems, noise and other factors determine that the annealing process will not always end to the lowest-energy state; instead, it becomes a sampling in the statistically important regions. This feature makes a potential application for the quantum annealers, since in classical statistic thermodynamics the approximation of important states is an important and useful approach.

To this end, the free energy in the grand canonical ensemble may be recast in an Ising-equivalent, quadratic unconstrained binary optimization (QUBO) model[27,28] as

$$Q = \lambda^T \mathbf{J} \lambda$$

$$\mathbf{J}_{m,m} = \Delta U_{corr,m} - kT \ln 10 \times \mathrm{pH} + \sum_{\substack{i\in m \\ j\in P}} f_{GB}(\Delta q_i, q_j) + \sum_{\substack{i\in m \\ j\in n}} f_{GB}(\Delta q_i, q_j^A)$$

$$\mathbf{J}_{m,n} = \sum_{\substack{i\in m \\ k\in n}} f_{GB}(\Delta q_i, \Delta q_k) \tag{13}$$

The matrix $\mathbf{J}$ is very similar to the coupling matrix of the corresponding Ising model. The QUBO model can then be sampled on quantum annealers to obtain important protonation states. Each run of the quantum annealer with the QUBO model returns a sample of protonation state $\{\lambda_1,\lambda_2,...,\lambda_N\}$ deemed to be most favorable at a given pH.

The pH titration of two protein systems is studied in this work (Figure 1). The first one is the acid-resistant, hyperstable Δ+PHS mutant of staphylococcal nuclease (SNase).[29] It contains 49 ionization side-chain groups without considering the terminuses, including 6 Asp, 11 Glu, 2 His, 7 Tyr, 18 Lys, and 5 Arg residues. The second one is α-lactalbumin,[30] which contains 41 ionization groups, including 13 Asp, 9 Glu, 2 His, 5 Tyr, 10 Lys, and 2 Arg residues. For both systems, the GB parameters, specifically the Born radii, are determined using the Still method[31,32] with the CHARMM22 force field.[33] To construct the pH titration curve of all groups, the protonation probability of each individual site is computed on classical computers or sampled on quantum annealers from pH 0.0 to 14.0 at an interval of 0.25.

On classical computers, the pH titration is determined with the exact partition function of the protein systems (eq 12) computed using all protonation states at each given pH state. The calculations are carried out using 1320 cores with the simple embarrassingly parallel scheme. We note that approximations could be made to approximate the partition function and accelerate the calculations, such as assuming one specific ionization state for these sites with a p*K*a value far away from the pH value. But this simplification will not fundamentally change the problem of a fast-growing number of states if a bigger protein molecule is studied.

For quantum annealer simulations, the $\mathbf{J}$ matrix (eq 13) is first computed with a negligible cost on classical computers for each pH value. The QUBO model is inputted to the D-wave

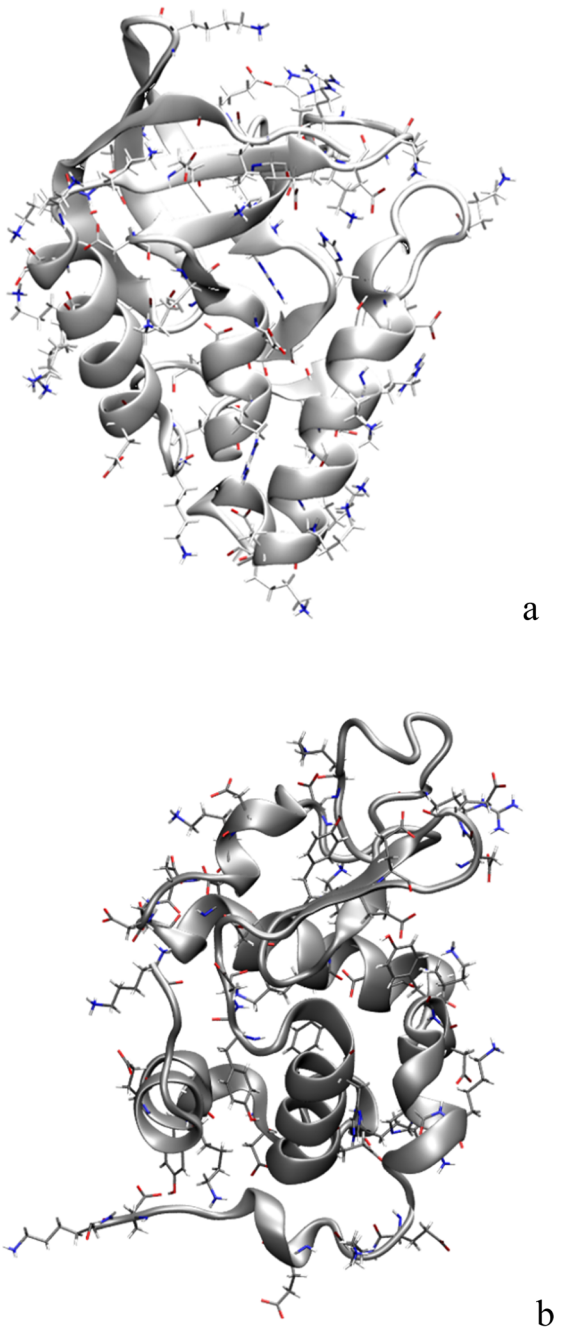

Figure 1. Structure of (a) staphylococcal nuclease, PDB ID 3bdc,[29] and (b) α-lactalbumin, PDB ID 1alc.[30] The ionizable groups are shown in balls and sticks.

Embedding Composite solver with the Advantage system 4.1[34] through the cloud computing platform,[35] which upon the completion of annealing process returns a favored protonation state as a sample. Multiple samples are needed to compute the approximate partition function and reconstruct the pH titration. Thus, the annealing process is repeated 20 times to obtain 20 protonation state samples for each pH. All unique protonation states forming the whole pH range are combined to compute the partition function and protonation probability (details in S.I.).

Table 1 compares the computational timing costs of classical computers and quantum annealers. For SNase and α-lactalbumin, computing the energy of all states to reconstruct

https://doi.org/10.1021/acs.jctc.3c00606
J. Chem. Theory Comput. 2023, 19, 5671−5676

Table 1. Comparison of Efficiency of Classical Computers and Quantum Annealers

System	Number of protonation states	Classical computer time[a]	Quantum annealer time[b]
staphylococcal nuclease	2^{49} = 562,949,953,421,312	128,000 CPU-h	<0.2 s
α-lactalbumin	2^{41} = 2,199,023,255,552	500 CPU-h	<0.2 s

[a]The time is mostly spent on computing the energy of all protonation states and converted to single-CPU core cost. [b]The time is total wall time of one annealing process, including wrapper layer and communication cost.

the exact partition function takes about 128,000 and 500 CPU-hours, respectively, on classical computers for one pH value. In comparison, each annealing sample on quantum computers takes less than 0.2 s, though multiple samples are required for each pH value due to the nondeterministic nature of quantum annealers. While the huge difference in computational timings must be understood in the proper context of different computing mechanisms, the size-independence is a clear advantage for quantum computing systems. Taking the crudest approximation, one could estimate that the quantum advantage emerges for systems with more than 18 ionization sites in the protonation problem, since $18 \approx 41 - \log_2 \frac{500\text{ h}}{0.2\text{ s}} \approx 49 - \log_2 \frac{128000\text{ h}}{0.2\text{ s}}$.

Figure 2 compares the titration curves of all ionizable groups of SNase obtained from calculations using classical computers and samples obtained from the D-Wave quantum annealers. The results using a total of 737 raw, unique states sampled by the quantum annealers show reasonably good agreement with the exact results (Figure 2b), with large deviations at the high pH range.

Figure 3 compares the titration curves of α-lactalbumin obtained from calculations using classical computers and samples obtained from the D-Wave quantum annealers. Unlike SNase, the results using a total of 928 raw, unique states sampled by the quantum annealer show great agreement with the exact results. Note that the agreement could be significantly improved if simple schemes are used to augment the sample size from quantum annealers, as shown in Figures S1 and S2.

To understand the difference between the results of SNase and α-lactalbumin, the rank of protonation states sampled by quantum computers is reported in Tables S1 and S2. A lower rank corresponds to a state with lower free energy and higher statistical weight, such that rank 0 is the state with the lowest free energy for a given pH value. For SNase, the most probable protonation state with the lowest rank (and free energy) is sampled by quantum computers in a broad pH region spanning between 0.0 and 10.0. But the samples at higher pH are less desirable as a quantum computer is not able to sample the most favorable states. In contrast, the sampled states of α-lactalbumin are most favorable or close to most favorable throughout the whole pH range. This is consistent with the quality of the pH titration curves reported in Figures 2 and 3.

The sampling differences between the two systems might be further attributed to the differences in the interactions in the two systems. Figures S3 and S4 report the density of states of the most probable 40,000 protonation states of each system at different pH values. Obviously, the density of states of α-lactalbumin does not show significant change throughout the whole pH range, but there are significant changes for the density of states of SNase in the pH range between 10.0 to 15.0. Specifically, the low-free-energy states of SNase become denser at these high pH ranges than they become at lower pHs. Denser states certainly would deteriorate the effectiveness of the annealing process, but this might be improved by adjusting the annealing parameters of the quantum annealers. Determining the best annealing scheme is mostly a trial-and-error process; as such, this topic is left to future study due to cost consideration. In general, we believe this is an issue that could be improved without much difficulty.

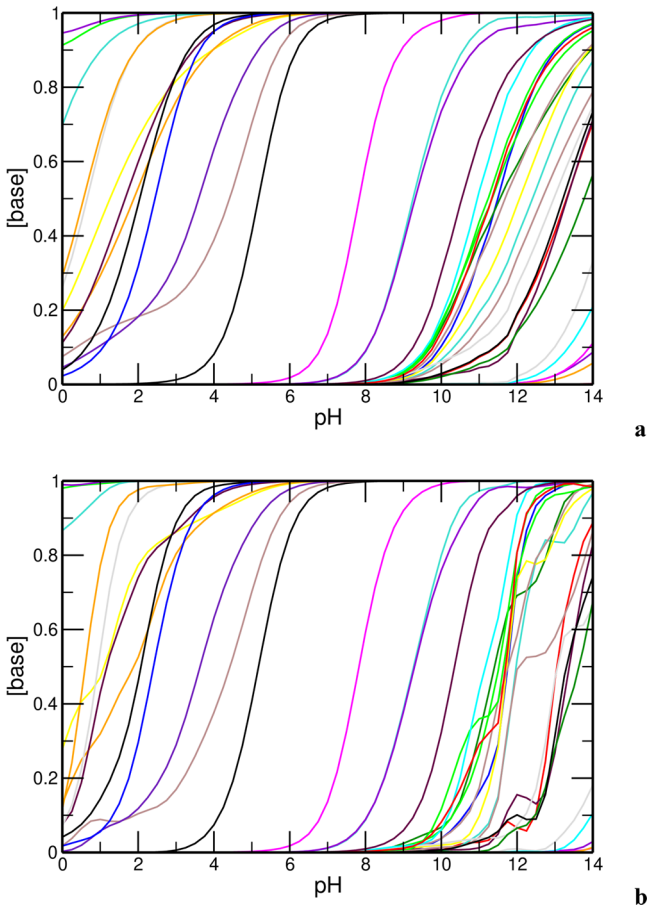

Figure 2. pH titration curves of staphylococcal nuclease. Results are from (a) classical computers with exact partition function; (b) quantum computers with 20 samples per pH.

We envision that the effectiveness of quantum computers in sampling statistically important states might be advantageous in future hybrid quantum/classical computing. One could use the classical computers to carry out data generation and sampling, while using quantum computers periodically to crack on different complex problems at other unconventional degrees of freedom and return the results to classical computers to continue. For the type of general ensemble simulations such as the concurrent protonation upon multiple sites, it might be feasible to use quantum computers as a Monte Carlo machine to quickly sample different protonation states, while using classical computers to provide accurate energy for the molecular system, as well as parameters for the models used in the quantum computers. This scheme becomes more and more feasible with both the improvement of the processing power and the reduced manufacturing cost of

https://doi.org/10.1021/acs.jctc.3c00606
J. Chem. Theory Comput. 2023, 19, 5671−5676

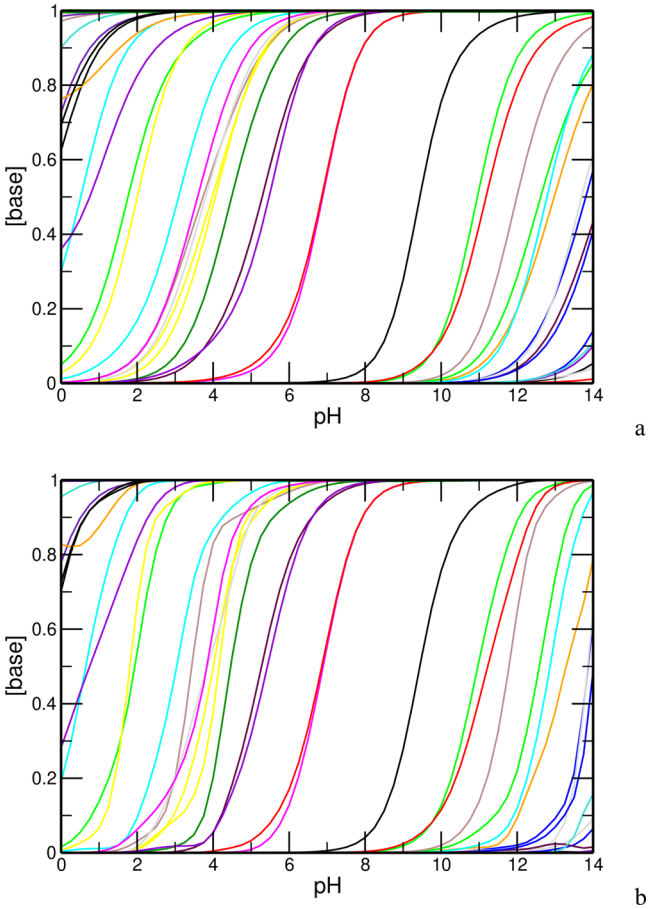

Figure 3. pH titration curves of α-lactalbumin. Results are from (a) classical computers with exact partition function; (b) quantum computers with 20 samples per pH.

quantum computers, as well as steady development in the quantum computing algorithms for many important chemistry problems.[36−38]

Development of the current quantum computers and computing technologies can be roughly divided into two classes based on their application targets: general-purpose, universal quantum computers, and special-purpose, quantum computers. The former is aimed to solve general problems in broad fields and developed on the foundation of unitary operator-based quantum logic gates;[39] the latter, in contrast, is designed to solve applications in relatively narrow fields − the D-Wave quantum annealers employed in the current work belong to this class. Much development effort in the chemistry field has been devoted to developing algorithms for general-purpose quantum computers to solve electronic structures, which is the ultimate goal of theoretical and computational chemistry. Relatively less attention has been paid to other problems using either general- or special-purpose quantum computers. Nevertheless, as we show here, many practical chemistry and biochemistry problems may also be good targets for the application of special-purpose quantum computers. The application of quantum computers to these problems, on one hand, could help researchers to cross the complexity barrier to study the chemistry problems at a higher level; while on the other hand, it would further help to accelerate the development of the whole quantum computing field.

In conclusion, we have demonstrated that, with a realistic physical model, quantum computers could be applied to the study of the protein ionization process as an efficient tool to sample the statistically important protonation states. The process of formulating the protonation free energy as an Ising model might be helpful for other problems in molecular processes. Similar techniques might be developed to allow more and more biomolecular processes such as protein folding or antibody design[40] to be studied using quantum computers.

■ ASSOCIATED CONTENT

Supporting Information

The Supporting Information is available free of charge at https://pubs.acs.org/doi/10.1021/acs.jctc.3c00606.

Theory for the development of the GB-based Ising model, quantum mechanical bonding correction term, reconstruction of pH titration; pH titration curves of staphylococcal nuclease and α-lactalbumin using augmented samples of quantum computer (Figures S1 and S2); density of states of staphylococcal nuclease and α-lactalbumin (Figures S3 and S4); sorted unique ranks of staphylococcal nuclease and α-lactalbumin sampled on quantum computer (Tables S1 and S2) (PDF)

■ AUTHOR INFORMATION

Corresponding Author

Hao Hu − *Department of Biochemistry and Biophysics, University of North Carolina at Chapel Hill, Chapel Hill, North Carolina 27599, United States; Polaris Quantum Biotech Inc., Durham, North Carolina 27701, United States;* orcid.org/0000-0002-6831-8352; Email: enzyme@gmail.com

Complete contact information is available at: https://pubs.acs.org/10.1021/acs.jctc.3c00606

Notes

The author declares no competing financial interest.

■ ACKNOWLEDGMENTS

We thank the research computing facility maintained by the UNC Office of Information Technology Services where all classical computations are painstakingly carried out. We appreciate the kind help from the Department of Biochemistry at UNC.

■ REFERENCES

(1) Junge, W.; Nelson, N. ATP Synthase. *Annu. Rev. Biochem.* **2015**, *84* (1), 631−657.
(2) Vinyard, D. J.; Brudvig, G. W. Progress Toward a Molecular Mechanism of Water Oxidation in Photosystem II. *Annu. Rev. Phys. Chem.* **2017**, *68* (1), 101−116.
(3) Warburton, R. E.; Soudackov, A. V.; Hammes-Schiffer, S. Theoretical Modeling of Electrochemical Proton-Coupled Electron Transfer. *Chem. Rev.* **2022**, *122* (12), 10599−10650.
(4) Agarwal, R. G.; Coste, S. C.; Groff, B. D.; Heuer, A. M.; Noh, H.; Parada, G. A.; Wise, C. F.; Nichols, E. M.; Warren, J. J.; Mayer, J. M. Free Energies of Proton-Coupled Electron Transfer Reagents and Their Applications. *Chem. Rev.* **2022**, *122* (1), 1−49.
(5) Zhou, H.-X.; Pang, X. Electrostatic Interactions in Protein Structure, Folding, Binding, and Condensation. *Chem. Rev.* **2018**, *118* (4), 1691−1741.

(6) Warshel, A.; Russell, S. T. Calculations of electrostatic interactions in biological systems and in solutions. *Q. Rev. Biophys.* **1984**, *17* (3), 283−422.
(7) Schönichen, A.; Webb, B. A.; Jacobson, M. P.; Barber, D. L. Considering Protonation as a Posttranslational Modification Regulating Protein Structure and Function. *Annual Rev. Biophys.* **2013**, *42* (1), 289−314.
(8) Onufriev, A. V.; Alexov, E. Protonation and pK changes in protein-ligand binding. *Q. Rev. Biophys.* **2013**, *46* (2), 181−209.
(9) Linderstrøm-Lang, K. U. On the ionisation of proteins. *C.R. Trav. Lab. Carlsberg* **1924**, *15* (1), 1−29.
(10) Božič, A.; Podgornik, R. Site Correlations, Capacitance, and Polarizability From Protein Protonation Fluctuations. *J. Phys. Chem. B* **2021**, *125* (46), 12902−12908.
(11) Khaniya, U.; Mao, J.; Wei, R. J.; Gunner, M. R. Characterizing Protein Protonation Microstates Using Monte Carlo Sampling. *J. Phys. Chem. B* **2022**, *126* (13), 2476−2485.
(12) Liu, Y.; Fan, X.; Jin, Y.; Hu, X.; Hu, H. Computing pKa Values with a Mixing Hamiltonian Quantum Mechanical/Molecular Mechanical Approach. *J. Chem. Theory Comput.* **2013**, *9* (9), 4257−4265.
(13) Li, G.; Cui, Q. pKa Calculations with QM/MM Free Energy Perturbations. *J. Phys. Chem. B* **2003**, *107* (51), 14521−14528.
(14) Hu, H.; Shen, L. In silico concurrent multisite pH titration in proteins. *J. Comput. Chem.* **2014**, *35* (20), 1491−1498.
(15) Mangold, M.; Rolland, L.; Costanzo, F.; Sprik, M.; Sulpizi, M.; Blumberger, J. Absolute pKa Values and Solvation Structure of Amino Acids from Density Functional Based Molecular Dynamics Simulation. *J. Chem. Theory Comput.* **2011**, *7* (6), 1951−1961.
(16) Baptista, A. M.; Teixeira, V. H.; Soares, C. M. Constant-pH molecular dynamics using stochastic titration. *J. Chem. Phys.* **2002**, *117* (9), 4184−4200.
(17) Lee, M. S.; Salsbury Jr, F. R.; Brooks III, C. L. Constant-pH molecular dynamics using continuous titration coordinates. *Proteins: Struct., Funct., Bioinf.* **2004**, *56* (4), 738−752.
(18) Mongan, J.; Case, D. A.; McCammon, J. A. Constant pH molecular dynamics in generalized Born implicit solvent. *J. Comput. Chem.* **2004**, *25* (16), 2038−2048.
(19) Lucas, A. Ising formulations of many NP problems. *Frontiers Phys.* **2014**, *2*, 5.
(20) Robert, A.; Barkoutsos, P. K.; Woerner, S.; Tavernelli, I. Resource-efficient quantum algorithm for protein folding. *npj Quant. Info.* **2021**, *7* (1), 38.
(21) Hermans, J.; Lentz, B. *Equilibria and Kinetics of Biological Macromolecules*; John Wiley & Sons, Inc.: NJ, 2013.
(22) Onufriev, A. V.; Case, D. A. Generalized Born Implicit Solvent Models for Biomolecules. *Annual Rev. Biophys.* **2019**, *48* (1), 275−296.
(23) Warshel, A. *Computer Modeling of Chemical Reactions in Enzymes and Solutions*; Wiley-Interscience: New York, 1991.
(24) de Falco, D.; Apolloni, B.; Cesa-Bianchi, N. A numerical implementation of quantum annealing. *Conference: Stochastic Processes, Physics and Geometry*; 1988.
(25) Apolloni, B.; Carvalho, C.; de Falco, D. Quantum stochastic optimization. *Stochastic Processes and their Applications* **1989**, *33* (2), 233−244.
(26) Kadowaki, T.; Nishimori, H. Quantum annealing in the transverse Ising model. *Phys. Rev. E* **1998**, *58* (5), 5355−5363.
(27) QUBO. https://en.wikipedia.org/wiki/Quadratic_unconstrained_binary_optimization (accessed 2023-08-04).
(28) Punnen, A. P. *The Quadratic Unconstrained Binary Optimization Problem*; Springer Cham: Switzerland, 2022.
(29) Castañeda, C. A.; Fitch, C. A.; Majumdar, A.; Khangulov, V.; Schlessman, J. L.; García-Moreno, B. E. Molecular determinants of the pKa values of Asp and Glu residues in staphylococcal nuclease. *Proteins: Struct., Funct., Bioinf.* **2009**, *77* (3), 570−588.
(30) Acharya, K. R.; Stuart, D. I.; Walker, N. P. C.; Lewis, M.; Phillips, D. C. Refined structure of baboon α-lactalbumin at 1.7 Å resolution: Comparison with C-type lysozyme. *J. Mol. Biol.* **1989**, *208* (1), 99−127.
(31) Still, W. C.; Tempczyk, A.; Hawley, R. C.; Hendrickson, T. Semianalytical treatment of solvation for molecular mechanics and dynamics. *J. Am. Chem. Soc.* **1990**, *112* (16), 6127−6129.
(32) Qiu, D.; Shenkin, P. S.; Hollinger, F. P.; Still, W. C. The GB/SA Continuum Model for Solvation. A Fast Analytical Method for the Calculation of Approximate Born Radii. *J. Phys. Chem. A* **1997**, *101* (16), 3005−3014.
(33) MacKerell, A. D., Jr; Bashford, D.; Bellott, M.; Dunbrack, R. L., Jr; Evanseck, J. D.; Field, M. J.; Fischer, S.; Gao, J.; Guo, H.; Ha, S.; Joseph-McCarthy, D.; Kuchnir, L.; Kuczera, K.; Lau, F. T. K.; Mattos, C.; Michnick, S.; Ngo, T.; Nguyen, D. T.; Prodhom, B.; Reiher, W. E.; Roux, B.; Schlenkrich, M.; Smith, J. C.; Stote, R.; Straub, J.; Watanabe, M.; Wiórkiewicz-Kuczera, J.; Yin, D.; Karplus, M. All-Atom Empirical Potential for Molecular Modeling and Dynamics Studies of Proteins. *J. Phys. Chem. B* **1998**, *102* (18), 3586−3616.
(34) The Advantage Quantum Computer | D-Wave. https://www.dwavesys.com/solutions-and-products/systems/ (accessed 2023-08-04).
(35) D-Wave Leap. https://cloud.dwavesys.com/ (accessed 2023-08-04).
(36) Cao, Y.; Romero, J.; Olson, J. P.; Degroote, M.; Johnson, P. D.; Kieferová, M.; Kivlichan, I. D.; Menke, T.; Peropadre, B.; Sawaya, N. P. D.; Sim, S.; Veis, L.; Aspuru-Guzik, A. Quantum Chemistry in the Age of Quantum Computing. *Chem. Rev.* **2019**, *119* (19), 10856−10915.
(37) Ma, H.; Liu, J.; Shang, H.; Fan, Y.; Li, Z.; Yang, J. Multiscale quantum algorithms for quantum chemistry. *Chem. Sci.* **2023**, *14* (12), 3190−3205.
(38) Blunt, N. S.; Camps, J.; Crawford, O.; Izsák, R.; Leontica, S.; Mirani, A.; Moylett, A. E.; Scivier, S. A.; Sünderhauf, C.; Schopf, P.; Taylor, J. M.; Holzmann, N. Perspective on the Current State-of-the-Art of Quantum Computing for Drug Discovery Applications. *J. Chem. Theory Comput.* **2022**, *18* (12), 7001−7023.
(39) Nielsen, M. A.; Chuang, I. L. *Quantum Computation and Quantum Information*; Cambridge University Press: New York, 2010.
(40) Khan, A.; Cowen-Rivers, A. I.; Grosnit, A.; Deik, D.-G.-X.; Robert, P. A.; Greiff, V.; Smorodina, E.; Rawat, P.; Akbar, R.; Dreczkowski, K.; Tutunov, R.; Bou-Ammar, D.; Wang, J.; Storkey, A.; Bou-Ammar, H. Toward real-world automated antibody design with combinatorial Bayesian optimization. *Cell Rep. Methods* **2023**, *3* (1), 100374.

https://doi.org/10.1021/acs.jctc.3c00606
J. Chem. Theory Comput. 2023, 19, 5671−5676